

# CALCULATIONS STRATEGIES TO FORECAST LIFETIME OF OXIDE/OXIDE COMPOSITE STRUCTURES UNDER COMPLEX LOADINGS

O. Sally<sup>1,2,3</sup>, C. Julien<sup>1</sup>, F. Laurin<sup>1</sup>, R. Desmorat<sup>2</sup> and F. Bouillon<sup>3</sup>

<sup>1</sup>ONERA, DMAS, Université Paris-Saclay, F-92322 Châtillon, France

Email : [orianne.sally@onera.fr](mailto:orianne.sally@onera.fr), [cedric.julien@onera.fr](mailto:cedric.julien@onera.fr), [frederic.laurin@onera.fr](mailto:frederic.laurin@onera.fr)

Web Page: <http://www.onera.fr>

<sup>2</sup>LMT, ENS Paris-Saclay/CNRS/Université Paris-Saclay, 61 avenue du Président Wilson, 94235 Cachan Cedex, France

Email : [desmorat@lmt.ens-cachan.fr](mailto:desmorat@lmt.ens-cachan.fr), Web Page: <http://lmt.ens-paris-saclay.fr>

<sup>3</sup>Safran Ceramics, Les cinq chemins, 33187 Le Haillan, France

Email : [florent.bouillon@safrangroup.com](mailto:florent.bouillon@safrangroup.com), Web Page: <http://www.safran-group.com>

**Keywords:** Composites; damage model; fatigue lifetime; cycle jumps

## Abstract

The present paper deals with an unified damage model able to predict the behaviour and damage evolution of oxide/oxide composites under static and fatigue loadings. It is formulated in a kinetic formalism that enables to handle real complex loadings. A cycle jumps method, that relies closely on the proposed damage evolution law is developed to reduce computational times during cyclic fatigue loadings and benchmarked against other methods available in the literature. The whole strategy is implemented in a FE code and allows fatigue simulation of composite parts.

## 1. Introduction

Due to their excellent mechanical properties at high temperatures, ceramic matrix composites (CMC) are interesting for applications in hot parts of engines. For some engine components subjected to moderate thermo-mechanical loadings (between 800 and 1000°C), oxide/oxide CMCs are potential candidate materials in regard to their interesting trade-off between mechanical properties, thermal stability and cost. One of their more interesting properties resides in the absence of physicochemical reaction with the environment over a large temperature range. Within this range, the non-linear response of this material is imputed exclusively to mechanical damage mechanisms. In this study, we focus on woven oxide/oxide composite and the fabric is a balanced eight-harness satin weave.

In order to design efficiently composite components, it is useful to propose a damage model able to predict the damage evolution during static and fatigue loading and to develop the associated computational strategy.

To fulfil these objectives, a specific damage model for this material has already been developed under static loadings [1] at Onera but remained to be extended to fatigue loadings. To our knowledge, there is no available damage model in the literature able to predict the fatigue lifetime of oxide/oxide materials. A Damage Model for Polymer Matrix Composites, developed at Onera (named ODM-PMC), was recently extended to cyclic fatigue loadings [2]. However, cyclic loadings are not representative of a real flight spectrum experienced during the entire lifetime of an aircraft. Fatigue models, using the so-called "kinetic damage evolution law" [3-7] allow to handle random complex loadings without using the notion of cycling, the damage law being written in a rate form  $\dot{d} = \dots$ . This work presents a unified damage model for woven oxide/oxide composites undergoing static and complex fatigue loadings. The model, described at the woven ply scale (mesoscale), is presented in section 2.

Moreover, particular attention has been paid to computational costs. Calculation strategies have been proposed in order to simulate large number of fatigue loading cycles of composite structures, particularly cycle jumps methods. Section 3 describes an innovative method of cycle jumps, relying closely on the model physics. This method is implemented in a finite element code and benchmarked against methods of cycle jumps available in literature [6,8-9].

## 2. Damage model

The model, expressed in the Continuum Damage Mechanics framework, describes the behaviour of oxide/oxide woven ply laminates, under static and complex fatigue loadings. Defined at the ply scale, this model is thermodynamically consistent. It is a unified continuum damage model able to predict the strength and the fatigue lifetime of composite materials. In order to be able to simulate real loadings, a kinetic (rate) formalism for the damage evolution law is preferred over a cyclic formalism. This approach allows to describe the temporal evolution of the mechanical properties of the composite. The difficulty is then to properly model the mean stress effect [4].

### 2.1. Macroscopic behaviour and damage mechanisms

The formulation of the present strain based damage model, is based on previous works performed at Onera and LMT Cachan for composites with polymer or ceramic matrix [1-3, 10], but takes into account the specifics of the studied oxide/oxide woven composite material. It is assumed that the observed non-linearities are only due to the following damage mechanisms (and damage variables  $d_k$ ):

- In-plane transverse cracking within the matrix in the warp (noted  $d_1$ ) and weft (noted  $d_2$ ) directions
- Yarn/matrix debondings (noted  $d_3$ )

The macroscopic behaviour, expressed in equation (Eq. 1), derives directly from the Helmholtz free energy.

$$\underline{\underline{\sigma}} = \underline{\underline{C}}^{\text{eff}} : (\underline{\underline{\varepsilon}} - \underline{\underline{\varepsilon}}^{\text{th}}) - \underline{\underline{C}}^0 : \underline{\underline{\varepsilon}}^r \quad \text{with} \quad \underline{\underline{C}}^{\text{eff}} = \left( \underline{\underline{S}}^0 + \sum_k d_k \underline{\underline{H}}_k \right)^{-1} \quad (1)$$

where  $\underline{\underline{\sigma}}$  is the stress tensor,  $\underline{\underline{C}}^{\text{eff}}$  the effective elastic stiffness tensor taking into account the effects of the two different damage mechanisms,  $\underline{\underline{C}}^0$  the initial elastic stiffness tensor,  $\underline{\underline{\varepsilon}}$  the total strain tensor,  $\underline{\underline{\varepsilon}}^{\text{th}}$  the thermal strain tensor, and  $\underline{\underline{\varepsilon}}^r$  the residual strain, described in section 2.3. In the present approach, the effects of damage mechanisms on the macroscopic behaviour are applied through the increase of the initial elastic compliance  $\underline{\underline{S}}^0$  with an additional term  $\sum_k d_k \underline{\underline{H}}_k$ , that depends on the damage variables  $d_k$  and the corresponding effect tensors  $\underline{\underline{H}}_k$ , describing the effects of an open crack on the effective stiffness.

The current rules of design for such composite structures use a criterion based on residual stiffness. This is why the criterion introduced is based on the damage evolution, which is directly linked to the stiffness evolution/one.

### 2.2. Damage evolution law

Ben Ramdane [1] demonstrated experimentally that the static damage in this material is mainly oriented by the microstructure due to the contrast of mechanical properties between the porous matrix and the fibers. Therefore, under plane stress hypothesis (representative conditions of the available tests and of the industrial applications), only two scalar damage variables,  $d_1$  and  $d_2$  are introduced next. Moreover, previous works on PMCs [11] showed that damage induced by static or fatigue loadings present the same damage pattern, effects on the behaviour and damage saturation level but have different evolution laws (damage induced by fatigue loadings evolves much more slowly than that

induced by static loadings). The same assumption is made for the studied material. Therefore, there is a unique damage evolution law for each damage mechanism, that merges the contributions from both static and fatigue loadings.

The driving forces  $y_k$  associated to the damage variables have been formulated in a so-called non-standard thermodynamic framework [2, 10]. For practical purpose, the driving forces are reformulated with equation (Eq. 2) as equivalent strains, homogeneous to strains.

$$\begin{cases} \varepsilon_{eq1} = \sqrt{\frac{2y_1}{C_{11}^0}} \\ \varepsilon_{eq2} = \sqrt{\frac{2y_2}{C_{22}^0}} \end{cases} \quad \text{with} \quad \begin{cases} y_1 = \frac{1}{2} \left( C_{11}^0 (\varepsilon_{11}^{d_1+})^2 + a_{26} C_{66}^0 (\varepsilon_{12}^{d_1+})^2 \right) \\ y_2 = \frac{1}{2} \left( C_{22}^0 (\varepsilon_{22}^{d_2+})^2 + a_{16} C_{66}^0 (\varepsilon_{12}^{d_2+})^2 \right) \end{cases} \quad (2)$$

They depend on (i) the different components of the initial elastic stiffness tensor  $\underline{C}^0$ , (ii) the parameter  $a_{16}$  (resp.  $a_{26}$ ) which couples damage induced in the warp (resp. weft) direction to in-plane shear and (iii) on the positive strains tensors  $\varepsilon^{d_k+}$  related to each damage mechanisms. The positive strains reported in equation (Eq. 2) correspond to the positive part, as proposed by [2], of the total strain tensor, where all the components are zeros except those inducing damage  $d_k$ .

The damage evolution laws of those two variables, expressed as a temporal differential equation (Eq. 3), are formulated as kinetic (rate) damage laws and derive directly from those described in [1-2]. They are based on the previous work performed by Angrand [3].

$$\begin{aligned} \dot{d}_k = & (d_{\infty k} - d_k) \left( \frac{\langle \varepsilon_{eqk}^{max} - \varepsilon_k^{0s} \rangle_+}{S_k} \right)^{s_k} \left\langle \frac{d}{dt} \varepsilon_{eqk}^{max} \right\rangle_+ \\ & + (d_{\infty k} - d_k)^{\gamma_k} \left( \frac{\langle \varepsilon_{eqk} - m_k \check{\varepsilon}_{eqk} - \varepsilon_k^{0f} \rangle_+}{S_k^f} \right)^{s_k^f} \left\langle \frac{d}{dt} \varepsilon_{eqk}^{max} - \frac{d}{dt} \varepsilon_{eqk} \right\rangle_+ \quad \text{for } k = [1,2] \end{aligned} \quad (3)$$

where  $d_{\infty k}$  corresponds to the saturation of the damage, ( $S_k, s_k$ ) and ( $S_k^f, s_k^f, \gamma_k$ ) are material parameters, which allow to calibrate respectively static and fatigue damage evolution laws. The parameters ( $\varepsilon_k^{0s}, \varepsilon_k^{0f}$ ) stand for the static and fatigue damage thresholds, where  $\langle \cdot \rangle_+$  is the classical Macauley brackets. The fatigue threshold  $\varepsilon_k^{0f}$ , that is lower than the static one, corresponds to the fatigue limit of the material.

To take into account the effect of the load ratio, a mean equivalent strain  $\check{\varepsilon}_{eqk}$  is introduced in the fatigue part of the damage evolution law. It is calculated thanks to an evolutive mean based on the whole history of loading and described in [3-4].

The evolution of  $\varepsilon_{eqk}^{max} = \max_{\tau} \varepsilon_{eqk}(\tau)$ , which is the maximum value of  $\varepsilon_{eqk}$  over the entire history of loading, allows to switch between the static and fatigue evolution, as illustrated in figure (Fig. 1). When the maximum load increases ( $\langle \frac{d}{dt} \varepsilon_{eqk}^{max} \rangle_+ > 0$ ), the static contribution is activated. Conversely, whenever the equivalent strain goes over the fatigue threshold, but does not reach a new maximum ( $\langle \frac{d}{dt} \varepsilon_{eqk}^{max} \rangle_+ = 0$ ), then only the fatigue contribution to damage evolution is active. For instance, during the first load increase in figure (Fig. 1),  $\varepsilon_{eqk}^{max}$  increases *i.e.* the first part of (Eq. 3) is activated and static damage evolves from the static threshold up to the peak load. During discharge, no damage is created. Then, during the loading phase of the second cycle, fatigue damage occurs once the fatigue threshold is reached ( $\varepsilon_{eqk}^{max}$  remains constant whereas  $\varepsilon_{eqk}$  increases: the second part of (Eq. 3) is thus activated). If  $\varepsilon_{eqk}$  ever exceeds the previous value of  $\varepsilon_{eqk}^{max}$ , as in the third cycle of (Fig. 1), then from this point upwards, the damage evolution is due to the static contribution of (Eq. 3). This kinetic formulation enables naturally the model to simulate any kind of loading, static, cyclic or spectral ones [3, 4].

It can be noted that the damage is only allowed to grow, in order to ensure the second principle of thermodynamics.

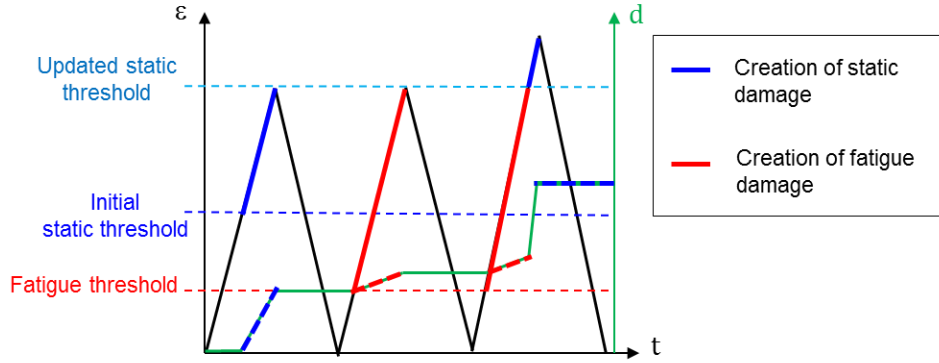


**Figure 1.** Evolution of the different damage contributions activated during cyclic or complex fatigue loading

### 2.3. Residual strains

The specific strain tensor  $\underline{\varepsilon}^r$  accounts for the residual strains after unloading that are due to the evolution of the different types of damage. Their growth rates are directly related to the damage variables, as shown in equation (Eq. 4).

$$\underline{\varepsilon}^r = \sum_{k=1}^2 [\chi_k e^{r_k d_k} \dot{d}_k R_k : e_k^*] \text{ with } e_k^* = \frac{\varepsilon^*}{|\max_t \varepsilon_{ki}^*|}, i = [1,2] \text{ and } R_k = \underline{\underline{H}}_k : \underline{\underline{C}}^0 \quad (4)$$

This formulation complies with the need of reducing computational cost at each increment, as it enables us to calculate analytically the residual strains, as proposed in [3].

### 2.4. Parameters identification

The fabric is supposed to be balanced and, in that regard, the warp and weft parameters are considered identical. The model was implemented on an integration point first in a home-made code. The parameters are identified by comparisons between tests and simulations made with this local model.

The static parameters,  $(S_k, s_k, \varepsilon_k^0)$  are identified on tensile incremental tests at  $0^\circ$ ,  $90^\circ$  and  $45^\circ$ . The identification is validated on off-axis tests ( $22.5^\circ$  and  $67.5^\circ$ ). The results of the identification on a Gauss point are illustrated by figure (Fig. 2) : panels (a) and (b) show the comparison between test results and numerical calculations during tensile incremental tests (static) at  $90^\circ$  and  $67.5^\circ$ .

In turn, the fatigue parameters  $(S_k^f, s_k^f, \gamma_k, m_k, d_{\infty k})$  are identified on a specific cyclic tensile test. This test consists of several stages of increasing applied maximal stress after a given number of cycles (around 1.8 million of cycles), with a constant stress ratio  $R_\sigma = \frac{\sigma^{min}}{\sigma^{max}} = 0.05$ . The figure (Fig. 2c) focuses on the degradation of the effective modulus (defined on panel (c)) throughout the three first stages.

Good agreement is found between the experimental data and the results of the simulations in term of non-linear behaviour, which confirmed the ability of the model to describe the macroscopic behaviour of laminated oxide/oxide materials.

To simulate the static behaviour of a representative volume element, the computation last a few seconds. As for fatigue loadings, it takes about one hour to compute a million cycles on a desktop computer.

## 2.5. Implementation in a FE code

In order to determine the behaviour of a composite part, the model is numerically implemented into an industrial finite element code through a user defined material subroutine. The tangent matrix is calculated analytically.

An application case simulating about 1000 cycles of imposed displacement in the warp direction on an open-hole plate is presented in section 3.2. The mesh includes 2500 elements. The computation time reaches 5 hours. The calculation costs remain too high for an industrial use in the case of fatigue polycyclic tests, if every single cycle among the millions of loading cycles are simulated for real composite parts.

As numerical simulations must be computationally efficient, calculation strategies have been investigated, in particular cycle jumps methods.

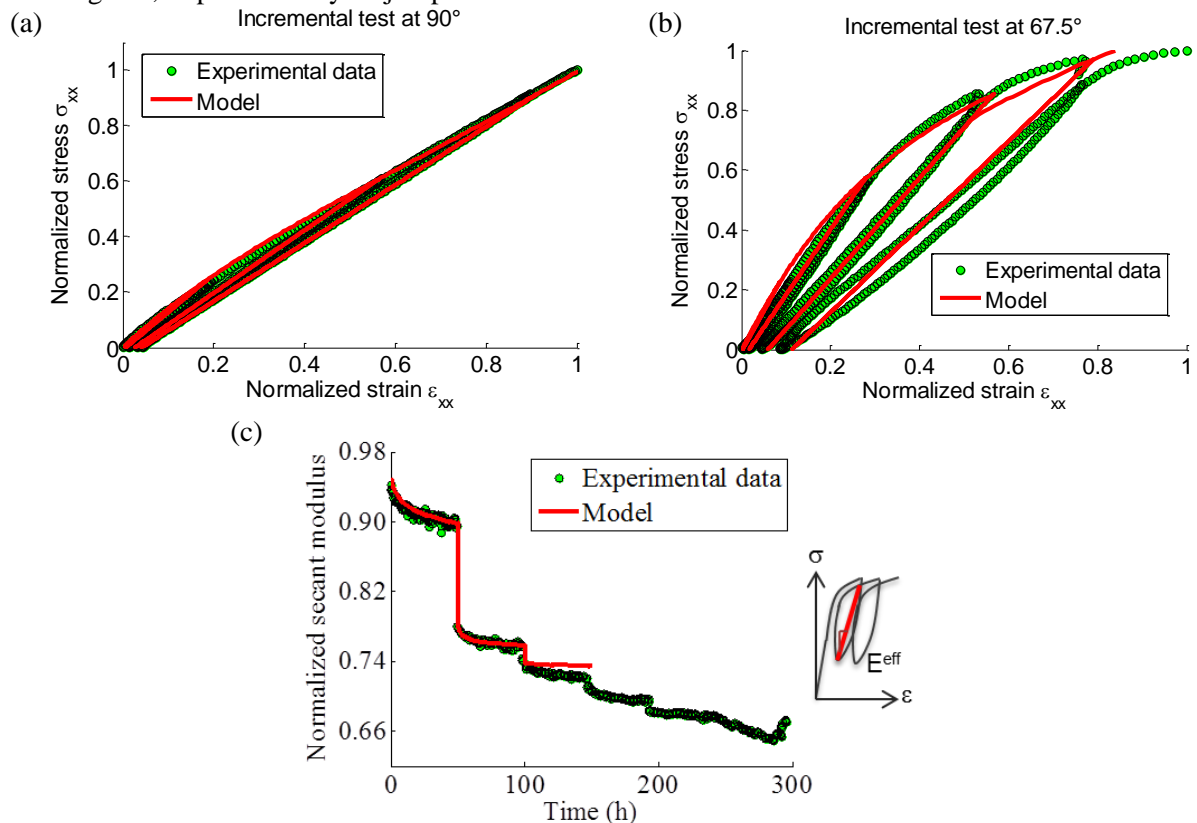


**Figure 2.** Comparison between model and experimental data on static (a), (b) and (c) fatigue tests

## 3. Cycle jumps technique

The concept of cycle jumps has been investigated by several authors [6,8-9,12]. The cycle jumps methods enable to reduce the number of cycles effectively simulated, by skipping over a large number of them. Consequently, it allows drastic reduction of computational costs for a given approximation of the final solution.

To alleviate that approximation, a new method of cycle jumps which relies closely on the model physics, is proposed in this section. This method is next benchmarked against a common scheme using an explicit Euler extrapolation. All simulations are compared to a reference calculation, where all cycles are conducted.

### 3.1. Principle

For the sake of clarity, the simulations are computed with a fixed jump length of  $\Delta N$  cycles. Let us consider  $d = d_1$  or  $d_2$  the matrix damage in one of the direction. The method for cyclic loading is

described in this section. Nevertheless, the same strategy can be applied to more complex periodic loadings, the notion of cycle being the unit loading pattern repeated over time. We point out that we only assume the periodicity of the applied loading, not of the material response.

### 3.1.1. Standard cycle-jump scheme

One of the simpler cycle-jump scheme is based on the extrapolation of damage variables by using an explicit Euler integration formula. Such a method has been used for metallic materials [6, 7] and then more recently for composite materials [2, 8]. It evaluates the local increase of damage for each integration point over each cycle jump of  $\Delta N$  cycles.

$$d_{N+\Delta N} = d_N + \left. \frac{dd}{dN} \right|_N \Delta N \quad (5)$$

Damage is assumed to evolve linearly during the jump with a rate equal to the increment of damage during the cycle preceding the jump. This assumption may not be accurate in our model, consequently an error directly related to the size of the jump is introduced.

### 3.1.2. Extrapolation scheme proposed

To reduce the induced error, a new method closely based on the form of the damage evolution law is proposed. The same formalism as for the damage evolution law is used during the jump. Static and fatigue damages evolve independently during a fatigue loading. Consequently, instead of calculating the increase of damage during a reference cycle, the increase of the static or monotonic (m) and fatigue (f) parts of damage are considered separately.

$$\begin{aligned} \dot{d} &= (d_\infty - d)\dot{m} + (d_\infty - d)^\gamma \dot{f} \\ \text{with } \dot{m} &= \left( \frac{\langle \varepsilon_{eq}^{max} - \varepsilon^{0s} \rangle_+}{S} \right)^s \left\langle \frac{d}{dt} \varepsilon_{eqk}^{max} \right\rangle_+ \\ \text{and } \dot{f} &= \left( \frac{\langle \varepsilon_{eq} - m\check{\varepsilon}_{eq} - \varepsilon^{0f} \rangle_+}{S^f} \right)^{s^f} \left\langle \frac{d}{dt} \varepsilon_{eqk}^{max} - \frac{d}{dt} \varepsilon_{eqk} \right\rangle_+ \end{aligned} \quad (6)$$

By integration of equation (Eq. 6) over one cycle, the current value of damage  $d$  being considered constant, the increment of damage over the reference cycle is obtained as:

$$\begin{aligned} \frac{dd}{dN} &= (d_\infty - d) \frac{dm}{dN} + (d_\infty - d)^\gamma \frac{df}{dN} \\ \text{with } \frac{dm}{dN} &= \int_{\varepsilon_{eq}^{max\ old}}^{\varepsilon_{eq}^{max}} \left( \frac{\langle \varepsilon_{eq}^{max} - \varepsilon^{0s} \rangle_+}{S} \right)^s \left\langle \frac{d}{dt} \varepsilon_{eqk}^{max} \right\rangle_+ \\ \text{and } \frac{df}{dN} &= \int_{\varepsilon_{eq}^{old}}^{\varepsilon_{eq}^{max\ old}} \left( \frac{\langle \varepsilon_{eq} - m\check{\varepsilon}_{eq} - \varepsilon^{0f} \rangle_+}{S^f} \right)^{s^f} \left\langle \frac{d}{dt} \varepsilon_{eqk}^{max} - \frac{d}{dt} \varepsilon_{eqk} \right\rangle_+ \end{aligned} \quad (7)$$

$\frac{dm}{dN}$  and  $\frac{df}{dN}$  represent respectively the increment of static and fatigue damage over the reference cycle. Those two quantities are considered constant during the cycle jumps. It is a strong hypothesis that will allow analytical calculation of damage variable, by integration of equation (Eq. 7).

Two cases are distinguished:

- If the simulation is strain-controlled fatigue, then no static damage is created ( $\frac{dm}{dN} = 0$ ). Moreover, the assumption is verified. Indeed, the equivalent strain remains constant if the equivalent strain is cyclic. Let us note that in this case the method is exact.
- On the contrary, with stress-controlled fatigue, the strain and consequently the equivalent strain mean increase, while it was considered constant during the jump.  $\frac{df}{dN}$  is then not constant over the jump and our approximation induces an error directly related to the span of the jumps.

Equation (Eq. 8) presents the two separate analytical solutions providing the damage value after the jump, depending on whether or not new static damage is created.

$$d_{N+\Delta N} = \begin{cases} d_{\infty} - \left[ -\Delta N (1 - \gamma) \frac{df}{dN} + (d_{\infty} - d_N)^{1-\gamma} \right]^{\frac{1}{1-\gamma}}, & \text{if } \frac{dm}{dN} = 0 \\ d_{\infty} - \left[ \exp\left(-\Delta N \frac{dm}{dN} (1 - \gamma)\right) \left( (d_{\infty} - d_N)^{1-\gamma} + \frac{df}{dm} \right) - \frac{df}{dm} \right]^{\frac{1}{1-\gamma}}, & \text{if } \frac{dm}{dN} > 0 \end{cases} \quad (8)$$

### 3.2. Benchmark between the different methods

These two methods are compared on an integration point on a million cycle stress imposed loading, with regards to a reference simulation. The reference represents a calculation where all the cycles have been computed thanks to the brute force of the kinetic (rate) model. Figure (Fig. 3a) represents the evolution of damage during a one million cycle fatigue test performed at a load ratio R=0.05 and figure (Fig. 3b) represents the error versus time of the computations. Let us note that the two methods converge towards the reference, but the convergence is faster with the novel method. Therefore, this method allows to run computationally cheaper simulations for a prescribed error or to obtain more precise results for a given computational cost, as illustrated in figure (Fig. 3b).

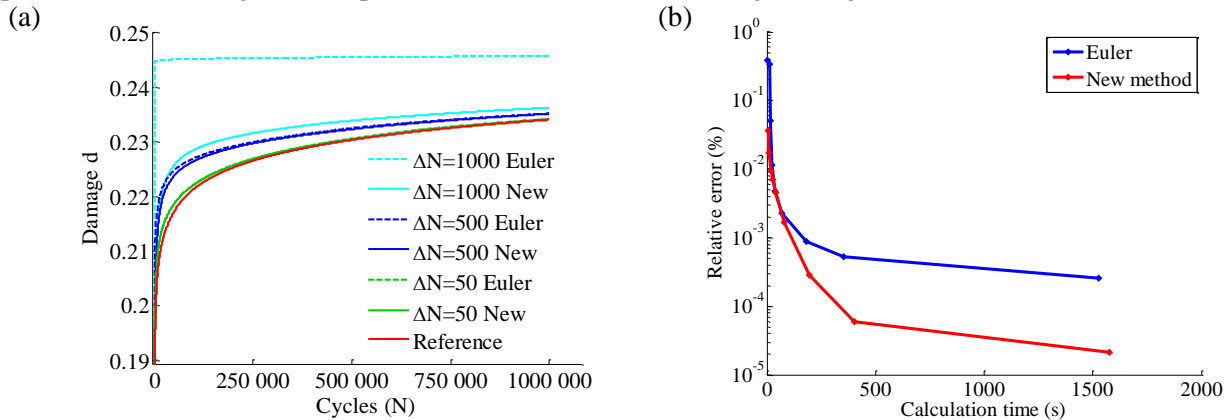


**Figure 3.** Comparison between explicit Euler scheme and the proposed cycle jumps method: (a) evolution of damage during the calculation and (b) relative error of damage versus calculation time.

The two methods have then been implemented in a finite element solver. The appeal of the proposed cycle jumps method is illustrated on figure (Fig. 4). Indeed, the simulation of an open-hole plate under a cyclic displacement is accelerated by a factor 60, with good precision on the damage evolution.

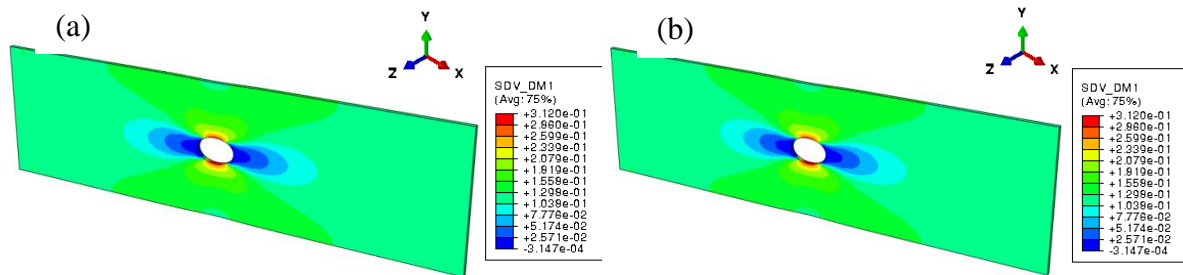


**Figure 4.** Comparison of simulations of open-hole plate subjected to a fatigue loading (1025 cycles at R=0.05 at imposed displacement), between (a) a full cycle-by-cycle computation (about 4.5 hours with 1 CPU) and a calculation with cycle jumps of size 100 cycles (5 min with 1 CPU)

#### 4. Conclusions and perspectives

To design oxide/oxide composite parts, it is necessary for the industrials to use physically based damage models, available in a finite element code. In that perspective, the proposed damage model allows to describe the evolution of damage under static and/or fatigue loadings and a first identification of its parameters has been performed on the woven oxide/oxide composite studied. The fatigue loading can be cyclic or spectral thanks to the kinetic formulation of the damage evolution law, which can naturally handle complex loadings. The calculation costs of fatigue tests remain too high for an industrial use in the case of fatigue polycyclic tests. This is the reason why the damage evolution law is associated to an efficient computational strategy of cycle jumps, in order to reduce the computational time (from 4.5 hours to 5 min in the example provided) and to allow considering large composite components. The model, as well as the numerical strategy associated, is implemented in a finite element code for large structural applications subjected to complex fatigue loadings.

#### Acknowledgements

The collaboration with SAFRAN Ceramics is gratefully acknowledged. This work was supported under PRC MECACOMP, French research project co-funded by DGAC and SAFRAN Group, piloted by SAFRAN Group and involving SAFRAN Group, ONERA and CNRS.

#### References

- [1] C. Ben Ramdane. Etude et modélisation du comportement mécanique de CMC oxyde/oxyde. *Doctorate thesis of Université de Bordeaux I*, 2014.
- [2] C. Rakotoarisoa. Prédiction de la durée de vie en fatigue des composites à matrice organique tissés interlock. *Doctorate thesis of Université de Technologie de Compiègne*, 2014.
- [3] L. Angrand. Modèle d'endommagement incrémental en temps pour la prédiction de la durée de vie des composites tissés 3D en fatigue cyclique et en fatigue aléatoire. *Doctorate thesis of Université Paris-Saclay*, 2016.
- [4] R. Desmorat, L. Angrand, P. Gaborit, M. Kaminski, et C. Rakotoarisoa. On the introduction of a mean stress in kinetic damage evolution laws for fatigue. *Int. J. Fatigue*, 77:141-153, 2015.
- [5] J. Lemaitre, J. P. Sermage, et R. Desmorat. A two scale damage concept applied to fatigue. *Int. J. Fract.*, 97: 67-81, 1999.
- [6] J. Lemaitre et I. Doghri. Damage 90: a post processor for crack initiation. *Comput. Methods Appl. Mech. Engrg.*, 115:197-232, 1994.
- [7] L. Gornet, H. Ijaz. A high-cyclic elastic fatigue damage model for carbon fibre epoxy matrix laminates with different mode mixtures. *Compos. Part B*, 42:1173:1180, 2011.
- [8] P. M. Lesne et S. Savalle. An efficient cycles jump technique for viscoplastic structure calculations involving large number of cycles. *2nd Int. Conf. on « Computational Plasticity » Models Software and Applications*, Barcelone, 1989.
- [9] W. Van Paepegem, J. Degrieck, et P. De Baets. Finite element approach for modelling fatigue damage in fibre-reinforced composite materials. *Compos. Part B Eng.*, 32: 575-588, 2001.
- [10] E. Hemon. Modèles multi-niveaux de prédiction des durées de vie en fatigue des structures composites à matrice céramique pour usage en turbomachines aéronautiques. *Doctorate thesis of Université de Bordeaux I*, 2013.
- [11] N. Revest. Comportement en fatigue de pièces épaisses en matériaux composites. *Doctorate thesis of École Nationale Supérieure des Mines de Paris*, 2011.
- [12] D. Cojocar, A. Karlsson. A simple numerical method of cycle jumps for cyclically loaded structures. *Int. J. Fatigue*, 28: 1677-1689, 2006.